COMPARATIVE STUDY: CFD ΔP VERSUS MEASURED ΔP FOR 30% FLEXIBLE DUCTS

Ahmet Uğursal
Ph.D. Student, Department of Architecture
Texas A&M University
College Station, TX

Charles Culp, Ph.D., P.E.
Associate Professor, Department of Architecture
& Associate Director, Energy Systems Lab
Texas A&M University
College Station, TX

ABSTRACT
This study modeled air flow and pressure drops in non-metallic flexible ducts using Computational Fluid Dynamic (CFD) analysis. CFD simulation results showed very close comparison with measured results. Flexible ducts can be installed in a variety of configurations with different compression. A configuration was specified for this study which focused on 30% compressed 5 foot-long flexible duct and 2 foot-long circular ducts placed on both ends. A CFD model was built and simulations were run under different volumetric air flows. The static pressure drop for those conditions were analyzed and displayed. The final CFD model is tuned until the closest results to the experimental data were achieved. In addition, an alternative duct configuration was tested for its potential to provide accuracy as a CFD model. The results will help define how to design and install flexible ducts so that pressure drop losses can be minimized for housing as code and above-code designs are implemented.

INTRODUCTION

Non-metallic flexible duct products have achieved wide usage in today's Heating Ventilating and Air-Conditioning (HVAC) applications, due to their advantages of cost and installation, over metallic ducts. Despite the advantages, an important factor in HVAC duct design is to attain minimum pressure loss throughout the distribution line. Compared to the straight ducts, the compression in flexible ducts results in increased pressure loss thus increased energy consumption. The ASHRAE Handbook – Fundamentals Chapter 35 (ASHRAE 2005) provides data on Pressure Drop Correction Factors based on the percent of compression extending to 30% (Figure 8, page 35.7). Abushakra et al. (2004) studied pressure drop inside fully stretched, 15% and 30% compressed flexible ducts In an existing research, Weaver and Culp investigated the pressure drop in flexible ducts for fully-stretched, and compression values of 4%, 15%, 30% and 45% (Duct Air Flow Study). In this study, we investigated the mesh configuration and generation method which represents the duct geometry and provides visual information on the flow patterns for 30% compressed flexible duct. Computational Fluent Dynamics (CFD) simulation packages were used for this purpose. Two alternative 3-D models were tested using CFD packages. The tested model, which provides less costly and faster results, is intended to be used for design purposes in the future.

METHODOLOGY

In this study, two commercial software packages were used to model and simulate the flexible duct. Gambit 2.2.30, which is the pre-processor for Fluent, was used to build the three-dimensional (3-D) computer model. Fluent 6.2.16 CFD software package was used to simulate the static pressure drop inside the flexible duct.

3-D computer model of 6" diameter flexible duct was generated for 30% compression in 5 ft. long. The laboratory data is based on in-H_20/100' standard. However, we used 5 foot-long model for the CFD simulations due to the limitations of the software and the computational capabilities of the supercomputer. A two-foot long circular section was added on both ends of the flexible duct to avoid placement of inlet and outlet boundary conditions in a turbulent area (Figure 1). This model corresponds with the board-supported configuration of the laboratory experiment, which has no sag. According to Gan and Riffat (1995) standard k-ε model is suitable to represent turbulence parameters of air, because air velocity inside the HVAC ducts is high which creates a turbulent flow. This semi-empirical model, in which kinetic energy (k) is derived from the exact equation, whereas the model transport equation for dissipation rate (ε) was obtained using physical reasoning, was used for the simulations of our study. In this standard k- ε model, it was assumed that the flow is fully turbulent, and the effects of molecular viscosity are negligible (Fluent 2005). A 'velocity inlet' boundary condition was used for the inlet. This allows defining flow velocity, and it is intended for incompressible flows. For the computations, corresponding air-velocity is used instead of air-volume (cfm). However, the results are presented in cfm. An 'outflow' boundary condition was used for the outlet, because the pressure for the exiting flow was not specified prior to the solution of the problem.

CFD simulations were conducted for 10 volumetric air flows, from 70 cfm to 160 cfm, in 10 cfm increments. Static pressure drop in 5 feet, 4 feet and 3 foot-long duct sections were derived. These data sets were multiplied by the factor of 20, 25 and 33.33 respectively to match with laboratory data of 100 foot-long duct. Simulation results were then compared to the laboratory data. In addition to this, an alternative duct configuration with a different end section was tested under the same conditions. The effects of the alternative configuration on the duct behavior were presented in comparison with the basic configuration.

Figure 1. Five-foot long flexible duct with two-foot long additions on both ends.

3-D MODELING OF DUCTS

The basic structure of flexible duct is composed of an embedded helix shaped steel wire, covered with a two-ply polyester membrane. For each 360° turn, helix core travels a distance of 1.5 inches along the central axis. This distance corresponds with the fully stretched configuration. In this study, 30% compression was modeled under blow-through conditions. This means that the duct wall is pressurized along the central axis.

The 3-D model consists of a center section, which is approximately 5 foot-long, and two end sections which are 2 foot-long each. The length of the central section for 30% compression is determined by multiplying the travel distance of one segment with an integer to have the closest value to 60 inches. Therefore, the center section has a length of 59.85 inches.

Gambit 2.2.30 was used to construct and mesh the model. The 3-D model of the flexible section is composed of individual surfaces of single 360° turn. Each single turn is composed of two half turns attached together. Half-turns were constructed by sweeping the profile arc along the half-turn helix (Figure 2). Desired length of flexible duct was obtained by multiplying individual surfaces as many times as necessary. Two two-foot long cylindrical volumes are attached to the flexible duct on both ends not to place inlet and outlet boundary conditions in a turbulent area (Figure 3).

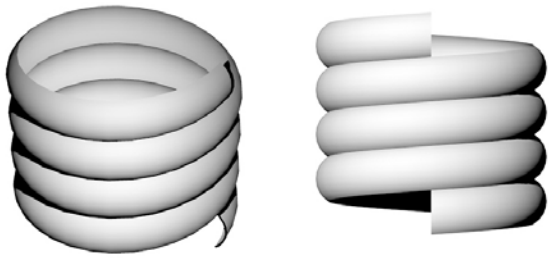

Figure 2. Structure of the flexible duct.

The alternative duct configuration consists of a straight inlet section which is identical to the first configuration. The outlet section, on the other hand, is cone shaped which starts with 6” ring and ends with 10” ring at the outlet (Figure 4). The same meshing algorithm was applied for both duct configurations.

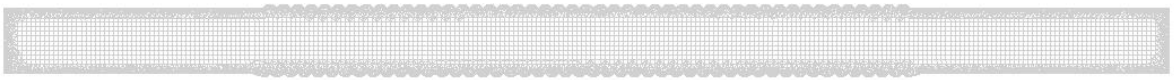

Figure 3. Basic Configuration of duct model and the meshing scheme.

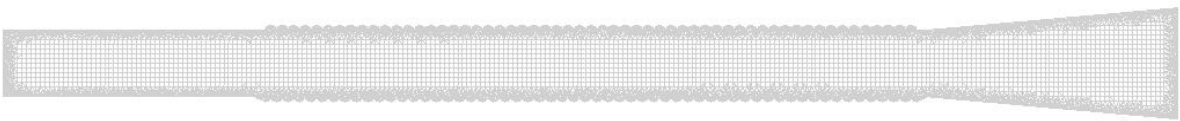

Figure 4. Alternative Configuration of duct model.

Meshing Algorithm

The 3-D model of the flexible duct consists mainly of curved surfaces with sharp angles between those surfaces. Structured grids failed to represent the blow through configuration of flexible duct without altering the geometry. Therefore, unstructured 'pave' face meshing scheme was first applied to ensure the geometric accuracy of the wall surface. Unstructured scheme provided enough flexibility for this purpose. The volume was then meshed using 'Hex/Core' scheme which creates a core of regular hexahedral elements surrounded by transition layers of tetrahedral, pyramidal, and wedge elements (Gambit 2004). This algorithm matched with the purpose of this study, which required a flexible scheme close to the flexible duct wall.

RESULTS

One important variable in CFD simulations, which affect the accuracy of the calculations, is the number of iterations. As presented in Figure 5, calculations become more stable on higher number of iterations. 100 and higher iterations showed close agreement within the flexible duct section, but differed in the end section. We used 130 and higher number of iterations throughout this study which well served our purposes of solving the flexible duct section accurately. This decision was taken based on the considerations of computation time and resources.

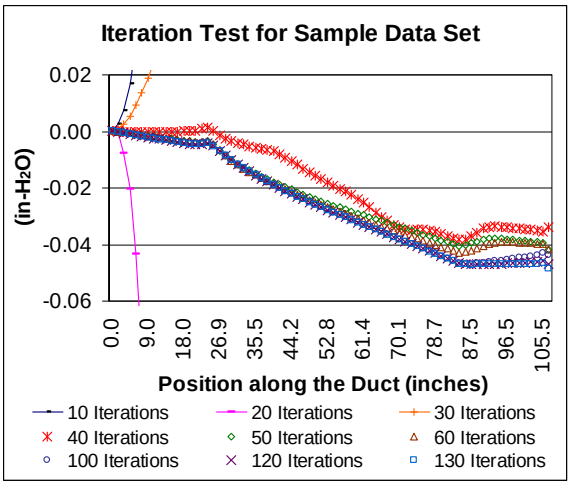

Figure 5. Iteration Test for a sample data set.

Static pressure data along the central axis was extracted from the simulation results and presented in Figure 6. This figure shows the static pressure change along the 5 foot-flexible-duct and 2 foot-straight end sections. As presented in Table 1, the static pressure difference (ΔP) in the flexible duct section varies between 0.030 and 0.143 for different air-volumes. ΔP for each air-volume was then multiplied by 20 to be able to compare the simulation results with the laboratory data.

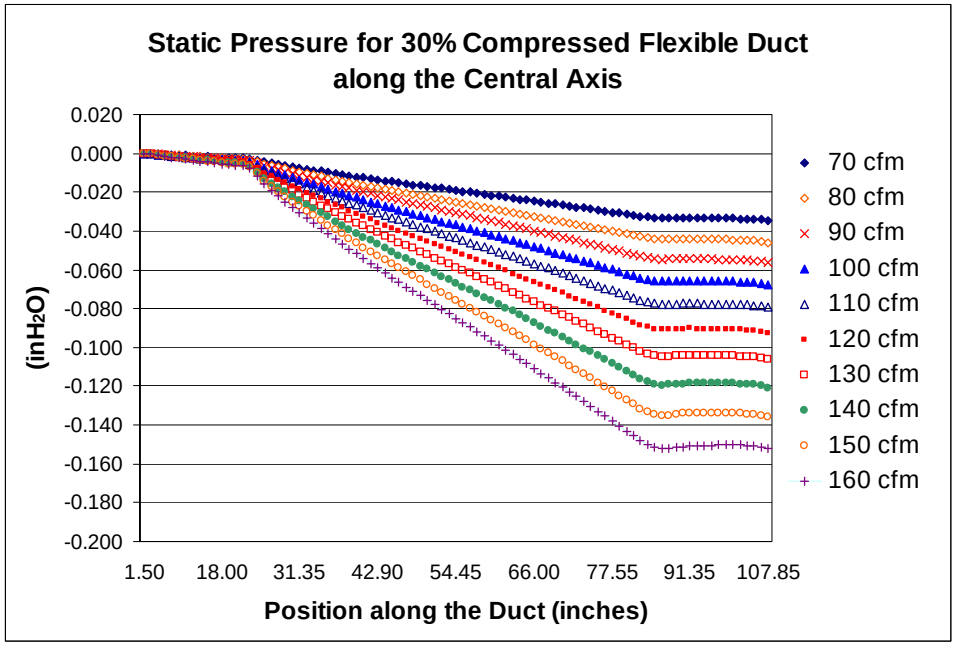

Figure 6. Static Pressure along the central axis of simulated duct model.

Table 1. Static pressure at 24 in. and 83.85 in. of central axis under various volumetric air-flows.

cfm	70	80	90	100	110	120	130	140	150	160
x=24.00	-0.003	-0.003	-0.004	-0.004	-0.005	-0.005	-0.006	-0.007	-0.007	-0.008
x=83.85	-0.033	-0.044	-0.054	-0.065	-0.077	-0.090	-0.104	-0.119	-0.134	-0.151
Pressure Difference in 5ft	0.030	0.041	0.050	0.061	0.072	0.085	0.098	0.112	0.127	0.143

Figure 7 shows the comparison of the simulation data to the laboratory experiments. As mentioned earlier, CFD simulation corresponds with the board supported configuration of the laboratory setting. As presented in Figure 7, CFD simulation shows close agreement with experimental data. Table 2 shows the numeric comparison of static pressure difference between experimental data and CFD simulation projected to 100 ft. Based on this comparison, it can be concluded that our CFD model tends to be more accurate on higher air volumes.

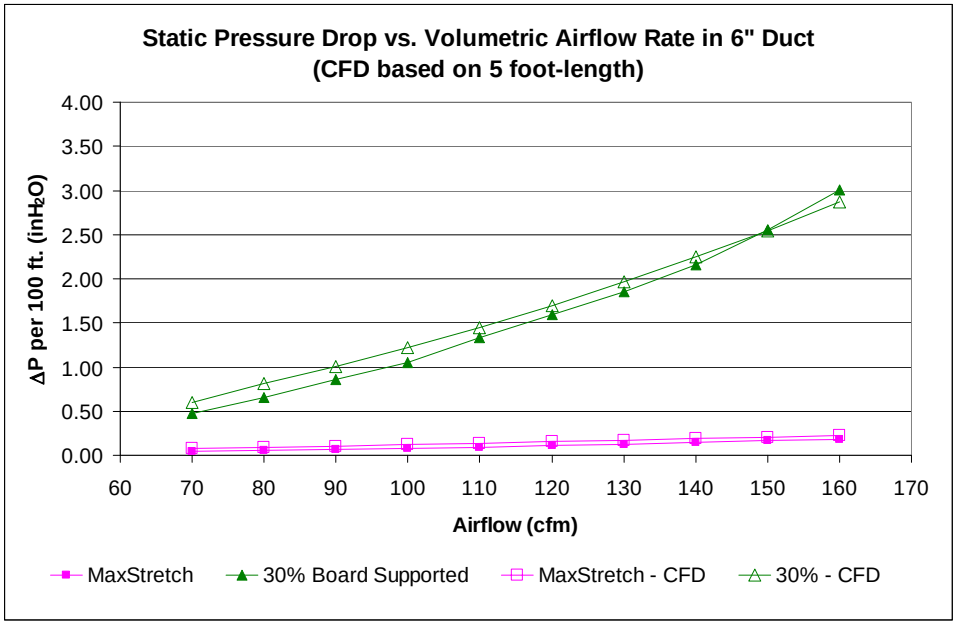

Figure 7. Comparison between CFD Simulation and Experimental Data.

Table 2. Static Pressure Drop (inH_2O) along 100 foot-duct-section based on CFD Simulation and Laboratory Experiments.

cfm	70	80	90	100	110	120	130	140	150	160
CFD Simulation	0.604	0.812	1.008	1.222	1.450	1.698	1.966	2.244	2.544	2.870
Experimental Data	0.470	0.650	0.856	1.051	1.332	1.596	1.855	2.159	2.552	3.010
Difference between CFD Simulation and Experimental Data	0.134	0.162	0.152	0.171	0.118	0.102	0.111	0.085	-0.008	-0.140

The accuracy of the CFD model was also tested based on three flexible duct sections, namely 3 ft., 4 ft., and 5 ft., extrapolated by the factor of 33.33, 25, and 20 respectively, to fit 100 feet configuration. Figure 8 shows the sections of the flexible duct used for this test. Static pressure difference between the two ends of each section was calculated for various air-volumes. The results are presented in Table 3 and Figure 9. According to these results, CFD simulation data based on 3 foot-duct-section showed the closest agreement with the experimental data.

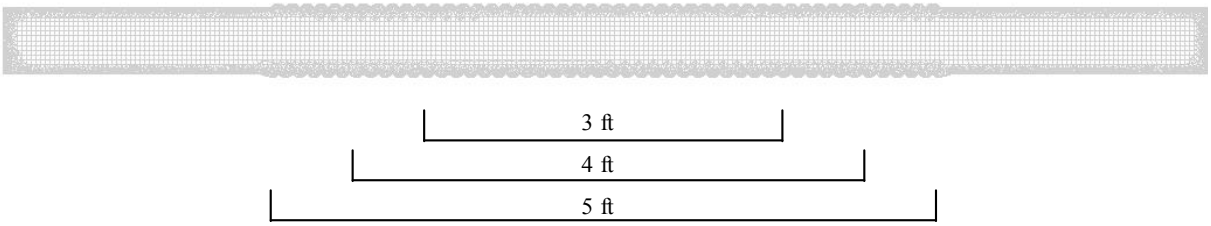

Figure 8. Three flexible duct sections used for comparison.

Table 3. Static Pressure Difference (inH_2O) of 100 foot-duct-section based on three flexible duct lengths.

cfm	70	80	90	100	110	120	130	140	150	160
Difference between CFD Simulation and Laboratory Experiment based on 5 ft. Data	0.134	0.162	0.152	0.171	0.118	0.102	0.111	0.085	-0.008	-0.140
Difference between CFD Simulation and Laboratory Experiment based on 4 ft. Data	0.115	0.138	0.122	0.131	0.070	0.042	0.040	-0.004	-0.109	-0.255
Difference between CFD Simulation and Laboratory Experiment based on 3 ft. Data	0.103	0.120	0.104	0.112	0.048	0.018	0.015	-0.036	-0.145	-0.293

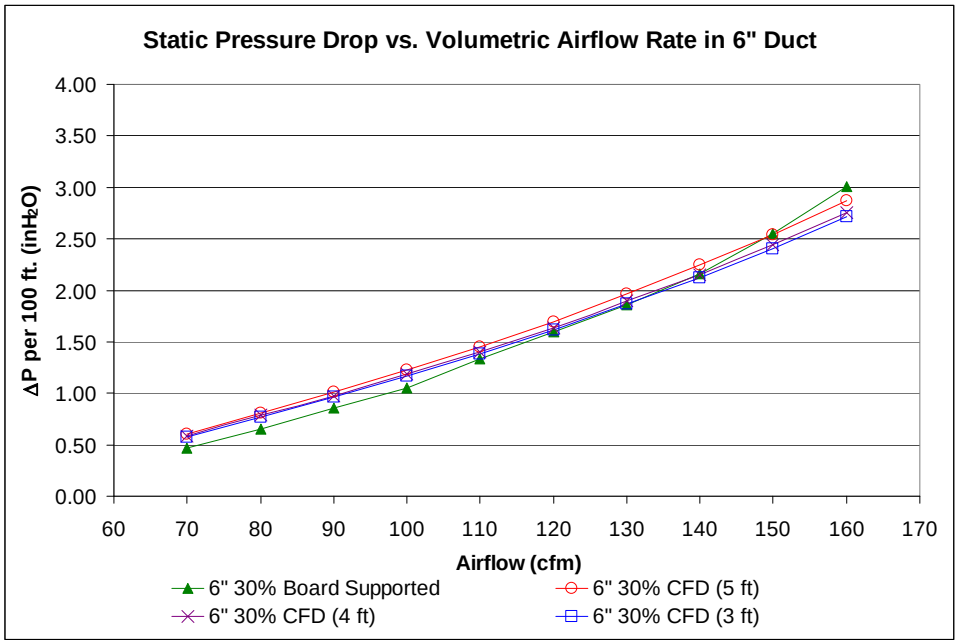

Figure 9. Static Pressure Difference extrapolated to 100 foot-long duct based on 3 ft., 4 ft. and 5 ft. long CFD simulation results.

An alternative duct configuration, which has a cone shaped end-section, was simulated to test its effect on the overall simulation. Air flows of 80 cfm, 120 cfm, and 160 cfm were chosen as sample cases to test alternative configurations effect on low, medium and high volumetric air flows. As shown in Figure 10, cone-shaped-end-section showed similar behavior throughout the flexible duct section for all three air-volumes. As presented in Table 4, it has very minor effect on the overall static pressure drop along the 5 ft. length. Table 4 shows the extrapolated results of 5 foot-long simulation to 100 foot-long standard data. The pressure difference in the end section is neglected because it does not affect the flexible section. It is concluded that the effect of cone-shaped end section is negligible for this particular study.

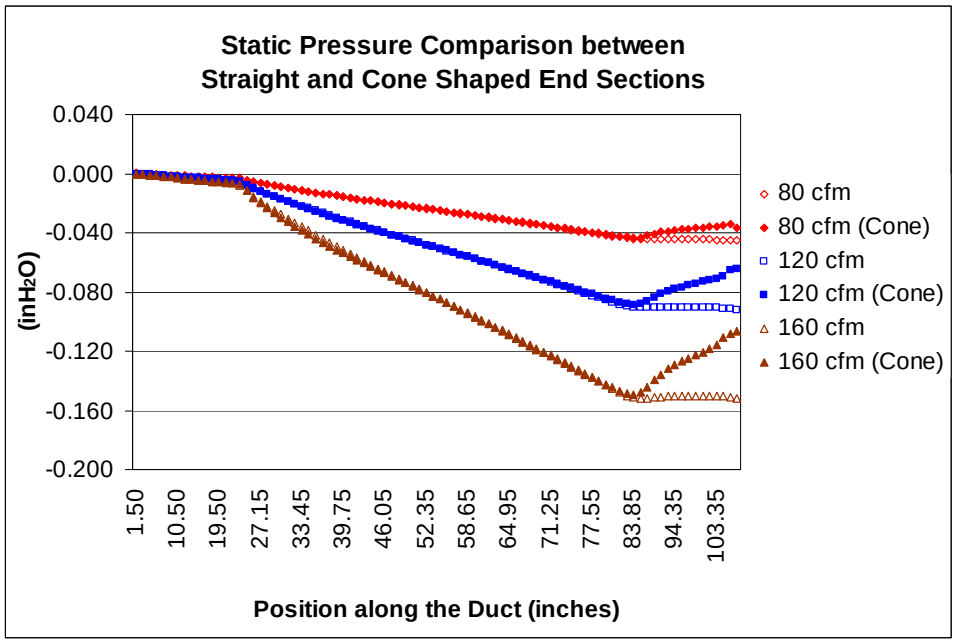

Figure 10. Comparison of Static Pressure change along the 5 foot-long duct between straight and cone-shaped end-sectioned CFD models.

Table 4. Static Pressure Difference (inH_2O) comparison between straight and cone-shaped end-sectioned models for 100 foot-duct-length.

cfm	80	120	160
CFD Simulation with Straight End-Section (based on 5 ft. Length)	0.812	1.698	2.870
CFD Simulation with Cone End-Section (based on 5 ft. Length)	0.797	1.662	2.834

CONCLUSION

CFD simulation results showed close proximity to the experimental result, although it consistently simulated higher pressure drop except 150 and 160 cfm. However, CFD model provided closer results on higher air volumes. It is concluded from the comparisons that calculations based on 3 foot-long section has the most accuracy compared to the 4 and 5 foot-long sections. This can be due to profile change after the 5 foot-long section. An alternative configuration was investigated to test this effect. The results from the alternative configuration showed very little variation compared to the initial configuration. However, alternative duct configurations such as trumpet-shaped inlet and outlet, which can provide smoother transition to and from the flexible duct, were still noted as future work. Finally, it can be concluded that our CFD model based on 3 foot-long section can be used for design purposes of board supported configuration of 30% flexible duct. At this point, a comparative study between CFD simulation and laboratory experiment of joist supported flexible duct configuration, which has sag, is also noted as future work.

REFERENCES

Abushakra, B., I. S. Walker, M. H. Sherman. 2004. *Compression Effects on Pressure Loss in Flexible HVAC Ducts*. International Journal of Heating, Ventilating, Air-Conditioning and Refrigeration Research, 10(3): 275 – 289.

ASHRAE. 2005. ASHRAE *Handbook of Fundamentals*. American Society of Heating Refrigerating and Air-conditioning Engineers, Atlanta, Georgia.

Fluent. 2005. Fluent 6.2 User's Guide, Fluent Inc., USA.

Gambit. 2004. Gambit 2.2.30 User's Guide, Fluent Inc., USA.

Gan, G. and S. B. Riffat. 1995. *k-factors for HVAC ducts: Numerical and Experimental Determination*. Building Services Engineering Research & Technology, 16(3): 133-139.

Weaver, K. and C. Culp, Private communication on study results which are submitted for publication.